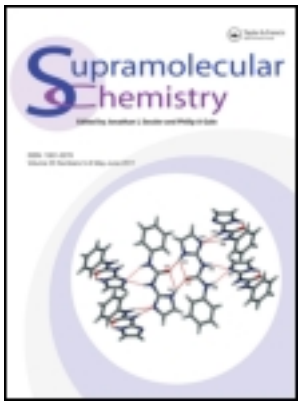

Supramolecular Chemistry
Publication details, including instructions for authors and subscription information:
http://www.tandfonline.com/loi/gsch20

Spontaneous self-assembly of aromatic cyclic dipeptide into fibre bundles with high thermal stability and propensity for gelation

T. Govindaraju [a]

[a] Bioorganic Chemistry Laboratory, New Chemistry Unit, Jawaharlal Nehru Centre for Advanced Scientific Research, Jakkur, Bangalore, 560064, India

Available online: 03 Nov 2011

To cite this article: T. Govindaraju (2011): Spontaneous self-assembly of aromatic cyclic dipeptide into fibre bundles with high thermal stability and propensity for gelation, Supramolecular Chemistry, 23:11, 759-767

To link to this article: http://dx.doi.org/10.1080/10610278.2011.628393

Supramolecular Chemistry
Vol. 23, No. 11, November 2011, 759–767

Spontaneous self-assembly of aromatic cyclic dipeptide into fibre bundles with high thermal stability and propensity for gelation

T. Govindaraju*

Bioorganic Chemistry Laboratory, New Chemistry Unit, Jawaharlal Nehru Centre for Advanced Scientific Research, Jakkur, Bangalore 560064, India

(*Received 3 August 2011; final version received 15 September 2011*)

Cyclic dipeptides (CDPs) are the simplest members of cyclic peptides exhibiting exceptional rigidity and stability. A detailed study on the spontaneous self-assembly of aromatic CDP (Phe-Phe) into fibre bundles with 1–2 μm thick and several millimetres long is described. These fibre bundles exhibit the structural hierarchy that is found in natural fibres such as spider silk and collagen. The solubility studies in various solvents provided more insights into the existence and nature of fibre bundles. Fibre bundles transform to gel in chloroform at critical concentration of added trifluoroacetic acid. Thermogravimetric analysis data indicated high thermal stability with multiple transitions attributed to the existence of structural hierarchy in fibre bundles. NMR studies revealed that aromatic π–π interactions along with intermolecular (N—H···O) hydrogen-bonded molecular chains are mainly responsible for the formation as well as observed high stability of fibre bundles. This detailed study of structural hierarchy, solubility, gelation and thermal stability demonstrates the robustness of aromatic CDP (Phe-Phe) to form fibre bundles.

Keywords: self-assembly; cyclic dipeptide; fibre bundle; molecular chain; gelation

Introduction

Self-assembly-based nano- and microstructures play an important role as the substitutes for various materials of biological origin, which are difficult to obtain in bulk quantity (*1–3*). In particular, peptide-based materials are of great interest due to their modularity, and many chemical modifications are possible to tune the structure and physicochemical properties (*4–15*). Polypeptides and proteins are the building blocks of a range of biological materials such as spider silk, collagen, actin and keratin (*16–19*). These materials have essential biological functions such as structural stability, mechanical (cytoskeletal) strength, self-defence and many other physiological functions. Fibrillar aggregates of polypeptides and proteins have also been implicated in various human diseases such as Alzheimer's, Parkinson's, type II diabetes and prion diseases (*20*). The reasons for studying peptide fibrillisation are of threefold: (i) to provide insight into the molecular mechanisms underlying the formation of fibrils, which are the main cause of various neurodegenerative disorders, (ii) to develop potential inhibitors to dissolve the fibrillar aggregates and (iii) to discover new synthetic peptide-based biomimetic materials that are the basis of study presented in this paper.

Molecular self-assembly driven by non-covalent interactions is the main driving force that Nature finally evolved to produce various forms of materials (*21*). Designing small organic molecules and peptides that undergo self-assembly to form fibres with properties comparable to natural fibres is of prime importance in the area of material science (*8*, *9*, *22*). These materials find applications as biomaterials and optoelectronic materials (*1–15*, *21–23*). Formation of various self-assembled structures such as nanotubes, nanofibres and nanospheres by cyclic and acyclic peptides has been reported (*4–12*). The π–π interactions between aromatic side chains of amino acids in polypeptides are known to induce peptide fibrillation (*24*). This process of fibrillisation can be utilised to develop novel biomaterials. An aromatic dipeptide (H-Phe-Phe-OH), the core recognition motif derived from β-amyloid peptide was shown to form nanotubes (*12*, *13*).

The cyclic dipeptides (CDPs) commonly referred to as diketopiperazines resulting from the condensation of two amino acids are very attractive scaffolds for designing variety of biomimetic materials (*25–28*). Their rigid cyclic structure and hydrogen bonding capability through *cis*-amides to form molecular chains or layers provide high stability to the derived biomimetic materials. The formation of microcapsules and molecular tapes in crystalline solid state by CDPs has been reported (*25–28*). Joshi and Verma (*29*) have reported the formation of fibres by cyclic (*L*)-Phe-(*L*)-Phe in their preliminary study. Recently, it has been reported that vapour deposition of the dipeptide NH_2-Phe-Phe-COOH at very high temperature

*Email: tgraju@jncasr.ac.in

ISSN 1061-0278 print/ISSN 1029-0478 online

http://dx.doi.org/10.1080/10610278.2011.628393
http://www.tandfonline.com

onto a substrate yields vertically aligned nanotubes. The chemical composition of these nanostructures was shown to consist of the corresponding CDP by mass spectroscopic analysis (*30*). We have recently reported the formation of 2D sheets with layered hierarchy similar to that of natural material such as graphene using CDP of unnatural amino acid phenylglycine (*31*).

In this paper, a straightforward route for the synthesis of (*LL*)- and (*DD*)-isomers of cyclo (Phe-Phe) under mild reaction conditions is presented. A detailed study of their molecular self-assembly to produce fibre bundles that resemble natural fibres and transformation of the fibre bundles into gel state using various microscopy techniques, thermogravimetric analysis (TGA), IR and NMR spectroscopy is described. This study significantly extends the preliminary results reported by Joshi and Verma (*29*) and our recent report on using CDP scaffolds as modular building blocks for designing self-assembly-based biomimetic materials (*31*).

Results and discussion

Synthesis of CDPs was achieved through a robust and straightforward synthetic route as shown in Scheme 1. Fmoc-(*L*)-Phe-OH was condensed with H-(*L*)-Phe-OMe using standard peptide coupling reagents to give the protected dipeptide Fmoc-Phe-Phe-OMe. The protected dipeptide was subjected to Fmoc-deprotection with 10% piperidine in dichloromethane. During this deprotection process, the dipeptide methyl ester undergo cyclisation to give CDP **1** in quantitative yield. Similarly, CDP **2** was obtained in good yield following the above procedure using (*D*)-phenylalanine derivatives. The earlier reports on the synthesis of CDPs rely on a Boc-deprotection strategy that involves harsh reaction conditions (*29*, *32*–*34*). The synthetic procedure reported here was carried out at ambient temperature and mild reaction conditions using Fmoc-chemistry protocols. Hence, this method is racemisation-free, straightforward and cost-effective. No tedious purification procedures are required. The CDPs spontaneously self-assemble to give insoluble fibres that were obtained with highest purity by simple filtration.

The CDP fibres were characterised by field emission scanning electron microscopy (FESEM), high-resolution transmission electron microscopy (HRTEM) and atomic force microscopy (AFM). Figure 1 shows the FESEM and HRTEM images of CDP **1** fibres. Formation of self-assembled fibres with thickness $\sim 1-2\,\mu m$ was observed (Figure 1(a)). The CDP fibres were of several millimetres long such that they are visible to the naked eye. The fibrous nature of the fibre bundles was confirmed by ion beam milling of an isolated fibre under a SEM (Figure 1(b)). The ion beam was directed to cut the fibre at a predetermined point. The cross section of ends resulting from the ion beam

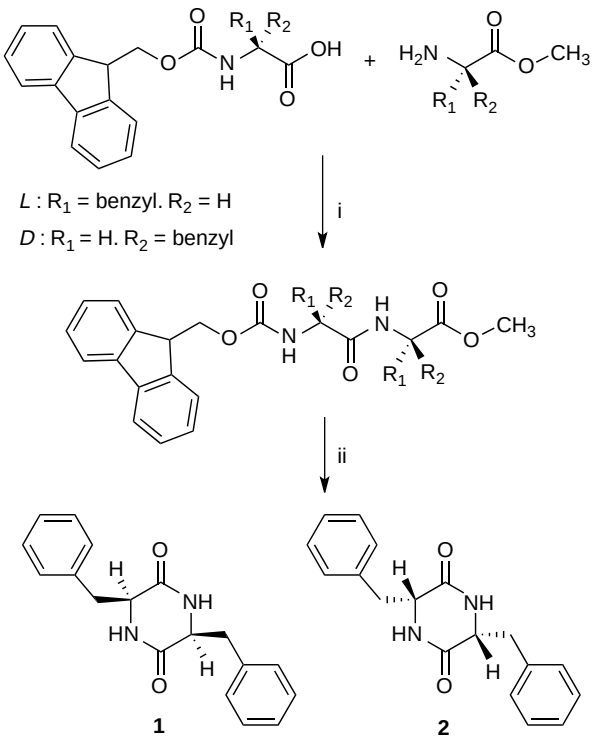

Scheme 1. Reagents and conditions: (i) EDC, HOBt, DIPEA, DCM, RT, 5 h. (ii) 10% piperidine in DCM, 2 h. EDC, 1-ethyl-3-(3-dimethylaminopropyl)carbodiimide; HOBt, 1-hydroxybenzo triazole; DIPEA, diisopropylethylamine; DCM, dichloromethane. (1) CDP Phe-Phe (CDP **1**), natural (*LL*)-isomer; (2) CDP Phe-Phe (CDP **2**), unnatural (*DD*)-isomer.

milling of fibre confirms its fibrous nature. FESEM data were further substantiated by HRTEM micrographs (Figure 1(c)). In addition, the HRTEM image indicated the bundle nature of CDP microfibres. CDP **2** (*DD*-isomer) was also found to form microfibres as shown in Figure 1(d). Furthermore, no significant changes in the morphology of the fibres formed by CDP **1** (*LL*-isomer) and CDP **2** (*DD*-isomer) and mixture of *LL*- and *DD*-isomers were observed (see Supplementary information). The CDP **1** and CDP **2** structures exhibit identical morphology as a result of self-assembly of CDPs through intermolecular (N—H$\cdots$O) hydrogen bonds to form linear molecular chains and subsequent aromatic $\pi-\pi$ interactions assisted linear self-organisation of molecular chains leads to the formation of microfibres.

To further understand the molecular mechanism and structural morphology underlying the formation of CDP **1** fibres, suitable solvent for dissolving fibres was sought. This search for suitable solvent revealed that organic solvents such as dichloromethane and chloroform can dissolve the fibres into clear solution upon acidification. The fibres were also found to dissolve in the fluorinated solvent such as 1,1,1,3,3,3-hexafluoro-2-propanol (HFP). However, fibres were insoluble in polar solvents such as methanol and water even after acidification. Only organic

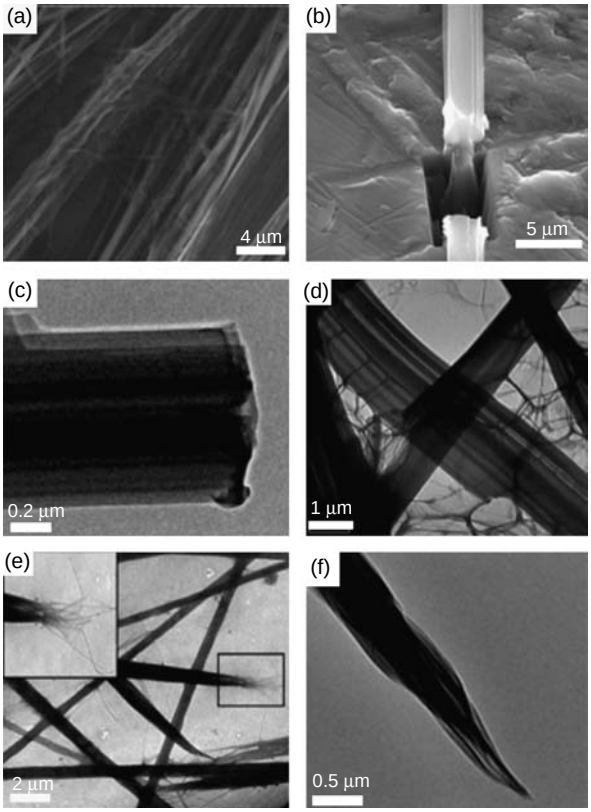

Figure 1. FESEM images of (a) CDP **1** suspended in dichloromethane, (b) an individual fibre was milled using ion beam, which confirms the fibrous nature of fibre bundle. HRTEM images of CDP **1** suspended in (c) dichloromethane, (d) CDP **2** fibres suspended in dichloromethane, (e) CDP **1** suspended in methanol acidified with acetic acid and the high-resolution image of a selected region (inset) to show the nanofibres project out at ends of fibre bundles and (f) high-resolution TEM image of a fibre bundle suspended in methanol acidified with acetic acid show the intertwined nanofibres.

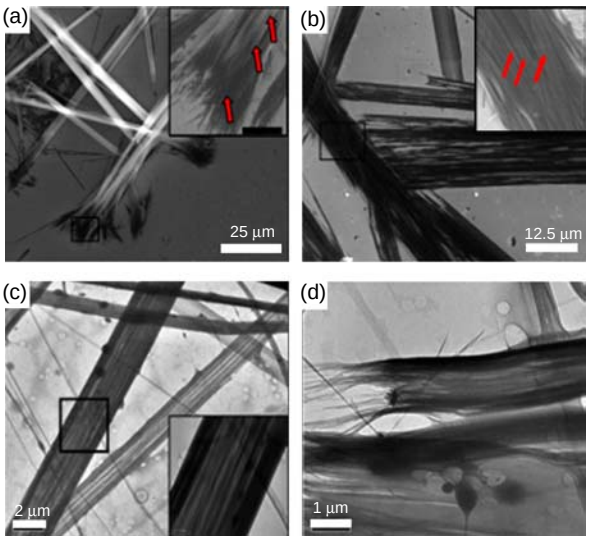

Figure 2. FESEM images of CDP **1** fibre bundles formed from its solution in (a) dichloromethane with acetic acid (inset: high-resolution image of the selected region shows that micrometer-sized fibres are a collection of self-assembled nanofibres and sub-micrometer fibres, arrows show the presence of hierarchy in the micrometer thick fibre bundle), (b) HFP (inset: high-resolution image of the selected region that shows fibre bundles are a collection of self-assembled nanofibres and sub-micrometer fibres, arrows point to nanofibres and sub-micrometer fibres that constitute the fibre bundle). HRTEM images of fibre bundles, (c) formed from the solution of CDP **1** in HFP. Inset: Expanded view of the selected region of a fibre bundle (square); (d) nanofibres project out at the ends of fibre bundles.

acids such as acetic acid and trifluoroacetic acid (TFA) were used to solubilise CDP fibres into organic solvents, and aqueous mineral acids were avoided as they may induce precipitation. These solubility experiments revealed in-depth knowledge about the formation of microfibres that are compact bundles of nano- and sub-micrometer fibres, as detailed below.

CDP **1** fibres remained as an insoluble suspension in methanol acidified with acetic acid. HRTEM data showed that the integrity of the fibres was retained except in their lengths (Figure 1(e)). The fibres length shortened due to the presence of acid and the bundle size remained intact. In addition, HRTEM data revealed that fibres are bundles of self-organised nanofibres as can be seen from the ends where the nanofibres clearly project out of the shortened microfibres (Figure 1(e), inset). HRTEM image in Figure 1(f) indicates the intertwined nature of the nanofibres to form fibre bundles. A similar observation was reported with collagen fibres on exposure to low pH which leads to partial disappearance of band pattern (*35*, *36*). Coexistence of short lengths of banded and long lengths of non-banded collagen revealed the presence of microfibrils and fibrils of collagen fibre (*35*, *36*). Next, the formation of fibre bundles from freshly prepared solutions of CDP **1** in dichloromethane–acetic acid (>6 μl/ml) and HFP were studied. The solutions of CDP **1** were drop coated on aluminium or silicon surfaces for FESEM and on holey carbon-coated copper grids for HRTEM. Fibre bundles formed spontaneously as the solvents evaporated on the surfaces. In the case of dichloromethane–acetic acid as a solvent, nanofibres and sub-micrometer fibres were seen at the ends of fibre bundles where fibre growth is abruptly stopped as a result of complete evaporation of the solvent (Figure 2(a)). Fibre bundles formed from the solution of CDP **1** in HFP also provided more insight into the hierarchy involved in the spontaneous self-assembly of CDP **1** similar to that of natural fibres. Spontaneous formation of fibre bundles with loosely assembled but still intact nano- and sub-micrometer fibres from the HFP solution was observed and there also exist some compact fibre bundles (Figure 2(b)). Solvent interaction with CDP molecule slows down the evaporation process and traces of residual solvent lead to the formation of loosely assembled

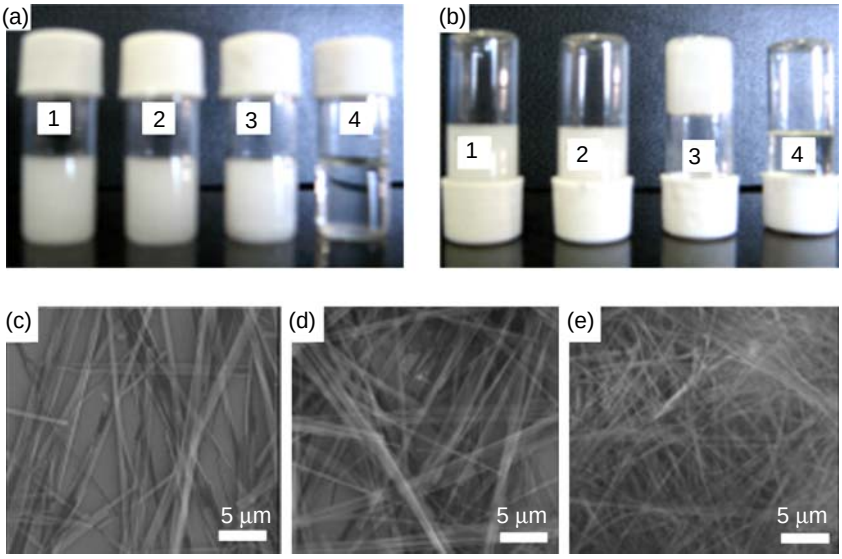

Figure 3. Gelation study. An equal amount of CDP **1** was suspended in 2 ml of chloroform (vials 1–4). (a) TFA was added to vials 1–4 in the order 1, 3.0 μl; 2, 6.0 μl; 3, 12 μl and 4, 24 μl. CDP **1** in vial 4 dissolve to give clear solution. (b) Vials 1–4 were allowed to stand overnight at room temperature. CDP **1** in vial 3 form fibrous gel. FESEM images of CDP **1** from vials 1–3 show the morphological changes occurred from suspension to fibrous gel: (c) vial 1, (d) vial 2 and (e) vial 3. In vial 3 (e), the fibrous gel contains fibres assembled in highly packed state.

fibre bundles. The nano- and sub-micrometer fibres formed from the HFP solution of CDP **1** as a result of diffusion limited solvent evaporation. In addition, partial hetero-molecular hydrogen bonding between CDP and HFP molecules on the fibre's surface and aromatic interactions support the formation of loosely bound fibre bundles. Nevertheless, these loosely assembled fibres revealed further insight into the understanding of the structural morphology and bundle nature of the CDP fibres. The spontaneous self-assembly of CDP **1** into fibre bundles from its HFP solution was also observed in the HRTEM images (Figure 2(c),(d)). AFM data further confirmed the aforementioned observations, as the structural topography and corresponding height profiles showed the presence of fibre bundles (see Supplementary Information).

The gelation propensity of CDP **1** in chloroform as a function of the concentration of TFA was assessed. Specifically, TFA was used because of the absence of methyl protons that is useful in comparative analysis of the data from other techniques. As shown in Figure 3(a), an equal amount of CDP **1** (2.5 mg/ml) was suspended in chloroform in vials 1–4. TFA was added to vials 1–4 in the order 3, 6, 12 and 24 μl/2 ml, respectively. CDP **1** in vial 4 dissolves immediately after the addition of TFA to give a clear solution while vials 1–3 remained suspensions. Vials 1–4 were allowed to stand overnight at room temperature. The CDP **1** in vial 3 transformed to fibrous gel, as confirmed by no free flow of suspension even after inverting the vial, while vials 1 and 2 remained suspensions (Figure 3(b)). This is an indicative of the critical concentration of TFA required for converting fibre bundle suspension in chloroform to a gel, above which CDP **1** dissolves to give clear solution and below which CDP **1** exists as free-flowing suspension. At critical concentration of added acid, gelation was presumably occurred due to the partial disruption of intermolecular (N—H···O) hydrogen bonds between CDP molecules in fibre bundles which leads to the altered network of homo- and hetero-molecular hydrogen bonding between CDP and TFA molecules. The fibrous gel is an intermediate state of CDP **1** between insoluble fibre bundle suspension and clear solution in chloroform upon the addition of TFA, which may be useful in processing fibre bundles for various applications. CDP **2** was also studied for its gelation propensity in chloroform. Similar to CDP **1** (*LL*-isomer), CDP **2** (*DD*-isomer) was transformed to gel in chloroform with the addition of TFA (6 μl/ml) and upon allowing the suspension to stand overnight at room temperature (see Supplementary Information). The study presented here is an example of utilising external stimuli to induce gelation. A similar study by Steed and coworkers (*37*) showed the transformation of a small molecule and $CuBr_2$ to metallogel by means of shear in the form of shaking. The formation of metallogel is attributed to the labile nature of coordination and hydrogen-bonded interactions. FESEM images provided clear insights into the morphological changes that occurred to the fibre bundles from its suspension to fibrous gel state in chloroform (Figure 3(c)–(e)). The fibre bundles start to organise into a close-packed arrangement with added TFA but are still in suspended form in vials 1 and 2. At critical concentration of TFA, i.e. in vial 3 the fibrous gel was found to contain fibres assembled in a highly packed gel state.

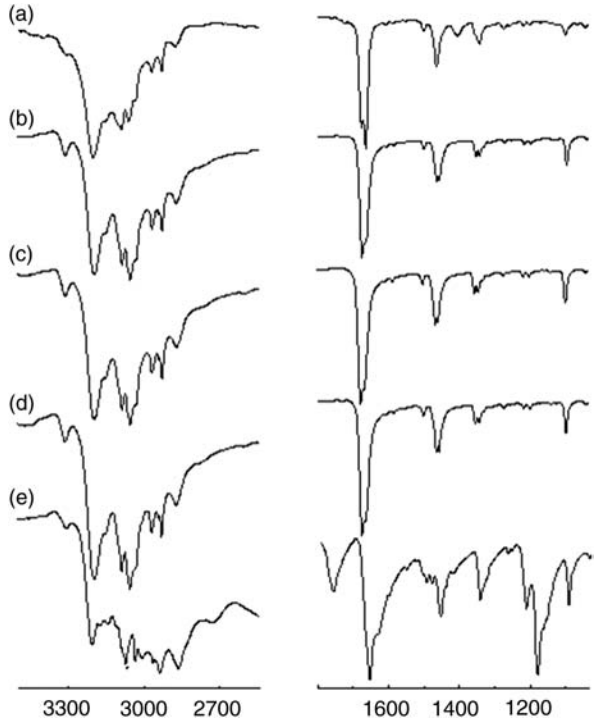

Figure 4. FT-IR spectra of CDP **1** as (a) solid, (b) suspension in chloroform, (c) suspension in chloroform +1.5 μl TFA, (d) suspension in chloroform +3.0 μl TFA and (e) suspension in chloroform +6.0 μl TFA (fibrous gel). Volume of TFA/1 ml of chloroform.

FESEM images further indicate that the fibres in the gel state appear thinner than those in the free-flowing suspension. Presumably, it is a result of the structures starting to disassemble at the surface leading to the formation of hetero-molecular hydrogen bonding network between CDP and TFA molecules in the gel state. Further addition of TFA beyond critical concentration resulted in complete disassembly of the structures to form clear solution due to complete disruption of (N—H···O) hydrogen bonds. This is a clear evidence for the hierarchical self-assembly present in CDP fibre bundles. These morphological changes to fibrous material were further confirmed by IR spectroscopy (Figure 4). Fourier transform infrared (FT-IR) spectra of CDP **1** solid, suspension and gel indicate the morphological changes occurred to fibre bundles during the transition of CDP suspension in chloroform to a fibrous gel state (vial 3). The changes were reflected in the region ~3300–3200 cm^{-1}, broadening and shifting of peaks between ~1680 and 1535, at 1457 and 1460 cm^{-1}. Appearance of new peaks at 1212 and 1180 cm^{-1} was also observed. All these changes were attributed to NH, amide I, amide II, aromatic C═C and ═C—H as a result of the variation in the hydrogen bonding and π–π interactions.

TGA was used to investigate the structural changes and stability in particular of the CDP **1** solid, suspension

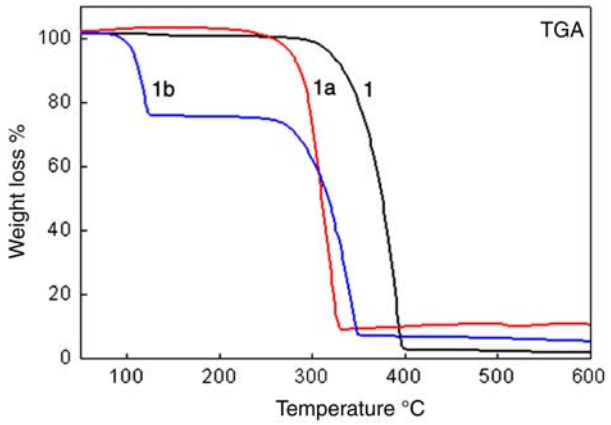

Figure 5. TGA. (**1**) CDP **1** fibre bundles (solid), (**1a**) CDP **1** fibre bundles suspended in chloroform (+3.0 μl TFA/2 ml), (**1b**) CDP **1** fibrous gel in chloroform (+12.0 μl TFA/2 ml).

and fibrous gel samples (Figure 5(a)). The CDP **1** solid, suspension and fibrous gel samples exhibited multiple transitions (see Supplementary Information). The CDP **1** solid showed major transitions at 324.9 and 390.8°C. The thermal decomposition temperature of 390.8°C clearly indicates the high stability of the fibre bundles. The acid-treated CDP **1** suspension (**1a**, TFA: 3 μl/2 ml) exhibited a relatively slight decrease in thermal stability with major transition temperatures at 100.3 (slight weight loss due to residual solvent), 263.4 and 295.6°C. However, the fibrous gel sample (**1b**) from vial 3 exhibited high thermal stability (342.4°C) but slightly less than CDP **1** solid sample. The relatively high stability of fibrous gel samples was accompanied by multiple transition temperatures at 121.2 (~25% weight loss due to solvent participation in gelation), 227.4, 297.6 and 342.4°C. These studies suggest that there is a clear change in the morphology of the fibre bundles as indicated by other techniques. Remarkably high stability observed with CDP **1** solid and fibrous gel accompanied by multiple transitions is attributed to the existence of fibre bundles.

The molecular mechanism underlying the formation of fibre bundles was supported by NMR studies. Dissolution of fibre bundles into monomeric CDP units was monitored by titrating the suspension of CDP **1** in $CDCl_3$ with TFA. Upon each addition of TFA (marked I–VIII in Figure 6) ^1H NMR spectra were acquired. In the fibre bundles, the amide proton (—NH) appeared at 5.64 ppm and such upfield shift was observed due to the location of amide proton (—NH) in the shielding zone of closely arranged aromatic rings (*31*, *38*). The amide proton (**a**) exhibited a overall downfield shift (2.35 ppm) upon the addition of TFA (I–VIII), which is attributed to the disruption of intermolecular hydrogen bonds (N—H···O) caused by the dissociation of fibre bundles into monomeric units. Thus, hydrogen bond interactions present in the fibre bundles are disrupted by the

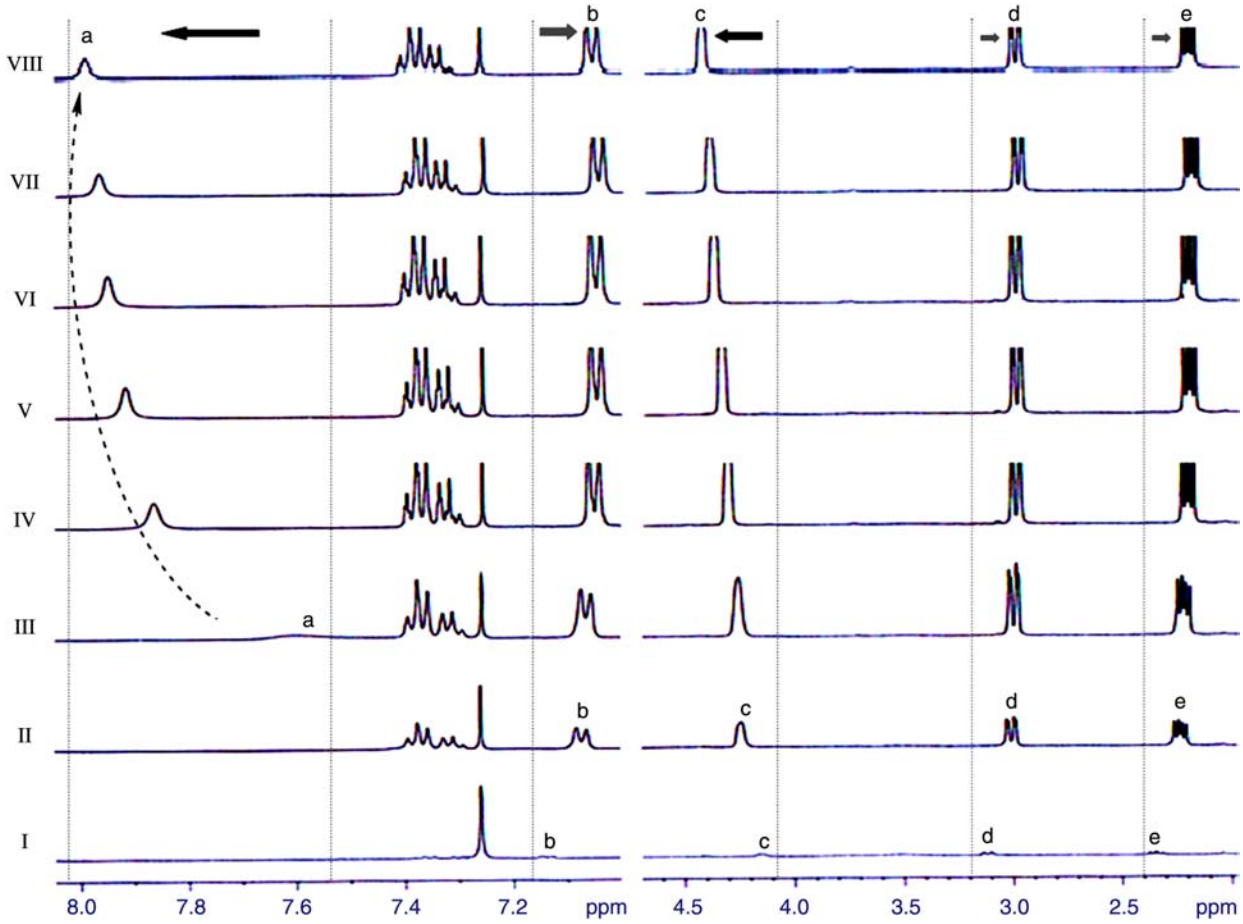

Figure 6. NMR characterisation of the fibre bundles. ^{1}H NMR spectra acquired at different additions of TFA. Spectra I–VIII corresponds to 0.0, 1.5, 3.0, 6.0, 12.0, 24.0, 48.0 and 96.0 μl additions of TFA, respectively. Chemical shift assignments of peaks are indicated: (a) H^{N} (amide NH), (b) aromatic protons (4H), (c) H^{α} (α-CH proton), (d,e) benzylic protons. Amide (H^{N}) appeared at 5.64 ppm before the addition of TFA (not shown in spectrum for better clarity of other peaks, see Supplementary Information) and shifted to 7.99 ppm downfield after adding TFA. For clarity, intensity of the spectral region 2.0–4.7 ppm magnified compare to the spectral region 7.0–8.1 ppm. Arrows indicate the direction of peaks shift upon addition of TFA.

addition of TFA. Similarly, downfield shift (0.28 ppm) of H^{α} proton (**c**) at 4.15 ppm was observed as expected. In contrast, four aromatic protons (**b**) in the region 7.10–7.17 ppm (spectrum I) exhibit further upfield shift (0.08 ppm) supporting the presence of aromatic interactions even at molecular state. A similar upfield shift (∼0.11 ppm) of benzylic protons (**d** and **e**) was observed. Spontaneous self-assembly of CDP molecules into fibre bundles can be further supported by considering non-covalent intermolecular interactions existing in the solid-state structure (*39*). The crystal structure clearly shows the existence of both hydrogen bonding and aromatic π–π interactions between CDP molecules (Figure 7) (*39*). Each CDP molecules can form pair of (N—H···O) hydrogen bonds to an adjacent molecule to form molecular chains. The intermolecular (N—H···O) hydrogen bonding extends the molecular chain in linear direction. The phenyl rings of hydrogen-bonded CDP molecules support self-organisation of molecular chains through aromatic π–π interactions to form nanofibres (Figure 7). Subsequently, the nanofibres undergo further spontaneous self-organisation through aromatic π–π interactions to produce sub-micrometer- and micrometer-thick fibre bundles.

Conclusion

In summary, this study demonstrated the spontaneous self-assembly of simple aromatic CDP (Phe-Phe) to form biomimetic fibre bundles. A straightforward synthetic route based on Fmoc-deprotection strategy was developed to access CDPs without involving cumbersome purification procedures. The structural hierarchy involves the nano- and sub-micrometer fibres that self-organise to form micrometer-thick and several millimetre long fibre bundles. The main strength of the work presented herein is the ability to achieve large-scale production of biomimetic CDP fibres compared to relatively inefficient biotechnology-based production of biological fibres. The structural hierarchy, solubility,

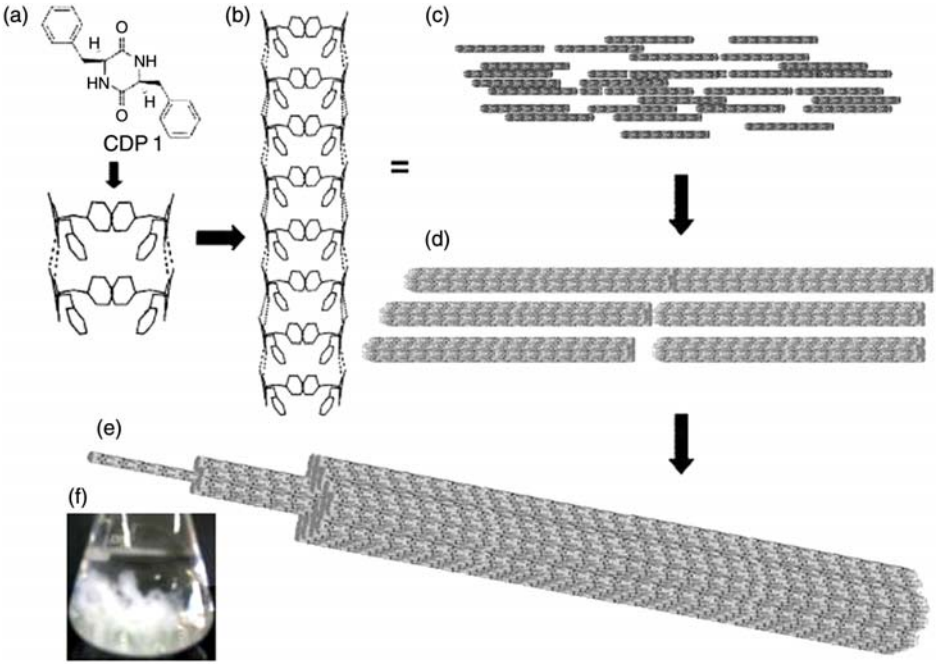

Figure 7. Molecular self-assembly of CDP **1** to fibre bundles. Crystal structure shows the molecular interactions between CDP **1** molecules (a, proposed based on Ref. (*39*)). The intermolecular N—H···O hydrogen bonding results in the formation of CDP molecular chains (b). The aromatic π–π interactions further stabilise the molecular chains to form nanofibres (c). These nanofibres spontaneously self-organise to form sub-micrometer fibres (d) and fibre bundles (e). CDP **1** fibre bundles suspended in dichloromethane (f, white fibrous material seen in conical flask).

stability, gelation and in particular employing intermolecular (N—H···O) hydrogen-bonded molecular chains along with aromatic π–π interactions to produce fibre bundles are useful in designing novel CDP-based biomimetic materials. For instance, fibre bundles of aromatic CDP with natural and unnatural amino acids can be viewed as potential candidates for the biomaterials applications such as neurological regeneration, organ replacement, production of suture and fabrics, optoelectronics and composite materials for high-performance materials.

Experimental

Materials and methods

All the solvents and reagents were obtained from Sigma-Aldrich (St Louis, MO, USA or Steinheim, Germany), and used as received unless otherwise mentioned. ^{1}H and ^{13}C NMR were measured on a Bruker AV-400 spectrometer with chemical shifts reported as parts per million (in $CDCl_3$/$CDCl_3$–TFA, tetramethylsilane as an internal standard). Mass spectra were measured on a Shimadzu GC-MS. IR spectra were recorded on a Bruker IFS 66/V spectrometer, using NaCl or as KBr pellet. TGA was carried out on a TGA 850 Mettler Toledo instrument. Elemental analysis was carried out on ThermoScientific FLASH 2000 Organic Element Analyzer and specific rotation $[\alpha]_D$ was recorded on a JASCO P-2000 polarimeter.

Synthesis of CDPs

9-Fluorenylmethoxycarbonyl-phenylalanine (Fmoc-Phe-OH) and phenylalanine methyl ester (H-Phe-OMe) were prepared by using standard protection protocols. Fmoc protected *L*/*D*-phenylalanylphenylalanine methylester (Fmoc-Phe-Phe-OMe) was prepared by standard peptide coupling procedures. Fmoc-Phe-OH (2.0 g, 5.16 mmol) was dissolved in dichloromethane, H-Phe-OMe (1.23 g, 5.67 mmol), 1-ethyl-3-(3-dimethylaminopropyl)carbodiimide (EDC.HCl, 1.19 g, 6.19 mmol), 1-hydroxybenzotriazole and (HOBt, 1.2 g, 6.19) were added. The solution was cooled on ice. Diisopropylethylamine (DIPEA, 2.14 g, 16.51 mmol) was added and the reaction mixture was stirred on ice for 1 h and then at room temperature for 5 h. The reaction progress was monitored by thin layer chromatography. The reaction mixture was evaporated to dryness and extracted from dichloromethane, washed with water and dried over anhydrous sodium sulphate. The solvent was evaporated to obtain Fmoc-Phe-Phe-OMe in quantitative yield.

*Synthesis of (3S,6S)-3,6-dibenzylpiperazine-2,5-dione (CDP **1**, LL-isomer)*

Fmoc-(*L*)-Phe-(*L*)-Phe-OMe (1.0 g, 1.82 mol) was subjected to Fmoc-deprotection in 10% piperidine/dichloromethane for 2 h. The reaction mixture was evaporated to dryness and

the residue was redissolved into dichloromethane. The CDP **1** spontaneously forms insoluble fibres. The suspension was filtered, washed with dichloromethane and methanol, and dried to obtain CDP **1** in quantitative yield. $[\alpha]_D^{24} = -115.0°$ ($c = 0.2$, CH_3COOH). ^1H NMR ($CDCl_3$–CF_3COOH, 400 MHz) δ_H 2.10–2.30 (q, 2H), 2.87–3.15 (dd, 2H), 4.29–4.48 (t, 2H), 7.01–7.14 (m, 4H), 7.27–7.52 (m, 6H), 7.80–8.14 (s, 2H), ^{13}C NMR ($CDCl_3$–CF_3COOH, 400 MHz) δ_C 39.7, 56.3, 128.4, 129.4, 129.8, 133.5, 170.0; anal. calcd (%) for $C_{18}H_{18}N_2O_2$. Found: C, 73.43; H, 6.19; N, 9.48; O, 10.90. Expected: C, 73.45; H, 6.16; N, 9.52; O, 10.87; GCMS: M/Z 294 [M^+]. Similarly (3*R*,6*R*)-3,6-dibenzylpiperazine-2,5-dione (CDP **2**, *DD*-isomer) was prepared following the procedure described for the synthesis of CDP **1**. $[\alpha]_D^{24} = +111.5°$($c = 0.2$, CH_3COOH). ^1H NMR ($CDCl_3$—CF_3COOH, 400 MHz) δ_H 2.14–2.28 (q, 2H), 2.88–3.09 (dd, 2H), 4.29–4.43 (t, 2H), 7.00–7.11 (m, 4H), 7.27–7.46 (m, 6H), 7.83–8.04 (s, 2H); ^{13}C NMR ($CDCl_3$-—CF_3COOH, 400 MHz) δ_C 39.6, 56.1, 128.2, 129.2, 129.7, 133.4, 169.6.

Field emission scanning electron microscopy

SEM measurements were carried out by using an FESEM, FEI Quanta 3D FEG microscope or FESEM, FEI Nova nanoSEM-600 equipped with field emission gun operating at 30 kV. Samples were prepared by placing an aliquot of the CDP suspension or solution on to a fresh, clean silicon surface, dried in the air before using the sample for analysis.

High-resolution transmission electron microscopy

Samples were prepared by placing a 10 μl aliquot of the CDP suspension or solution on a 200 mesh holey carbon supported copper grid. After removing excess fluid, the sample was dried at room temperature to remove the solvent. HRTEM images were obtained with a JEOL JEM 3010 electron microscope operating at 300 kV.

Atomic force microscopy

AFM measurements were carried out on a Veeco diInnova SPM operating in tapping mode regime. The samples prepared by drop casting CDP suspension or solution on a fresh, ultra clean silicon substrate, dried in air and used for AFM studies.

Fourier transform infrared spectroscopy

IR spectra of CDP **1** solid, suspension, gel and solution in chloroform were recorded on NaCl or as KBr pellet on a Bruker IFS 66v/S FT-IR spectrometer. The spectra were corrected for chloroform, NaCl and KBr.

Thermogravimetric analysis

TGA was carried out on a Mettler Toledo TG-850 instrument under flowing nitrogen atmosphere (40 ml min^{-1}) at a heating rate of 10°C min^{-1}, with total temperature range of 30–700°C. The CDP **1** suspended and solution samples were dried at room temperature before subjecting to TGA analysis.

Gelation experiments

CDP **1** (2.5 mg/ml) was suspended in chloroform at 25°C in four vials. TFA was added in increasing concentration. The samples were stored overnight at room temperature. No flow of solvent when the sample vials were tilted confirmed gel formation. The morphological changes in the fibre bundles upon the addition of TFA and subsequently the critical concentration of TFA at which gelation occurs were studied by FESEM, IR spectroscopy and TGA.

NMR spectroscopy

NMR experiments were carried out at 25°C on a Bruker Av-400 MHz spectrometer. Five milligram sample (CDP **1**) consisting of the fibre bundles was added to 500 μl $CDCl_3$ and transferred to a 5 mm NMR tube. The ^1H NMR spectra were acquired with 16 scans per FID. The formation of monomeric peptide units was monitored by titrating a suspension of fibre bundles of CDP **1** in $CDCl_3$ with TFA until complete dissolution was obtained. Upon each addition of TFA, ^1H NMR spectra were acquired.

Acknowledgements

Author thanks Prof. C.N.R. Rao, FRS for constant support and encouragement, JNCASR and Department of Biotechnology (DBT), India, for providing financial support through IYBA 2011; Prof. Vinod Subramaniam for critical reading of the manuscript; reviewers for their critical comments and suggestions which helped in improving the quality of the paper.

References

(1) Lutolf, M.P.; Hubbell, J.A. *Nat. Biotech.* **2005**, *23*, 47–55.
(2) Chai, C.; Leong, K.W. *Mol. Ther.* **2007**, *15*, 467–480.
(3) Place, E.S.; Evans, N.D.; Stevens, M.M. *Nat. Mater.* **2009**, *8*, 457–470.
(4) Ghadiri, M.R.; Granja, J.R.; Milligan, R.A.; McRee, D.E.; Khazanovich, N. *Nature* **1994**, *366*, 324–327.
(5) Bong, D.T.; Clark, T.D.; Granja, J.R.; Ghadiri, M.R. *Angew. Chem. Int. Ed.* **2001**, *40*, 988–1011.
(6) Hartgerink, J.D.; Beniash, E.; Stupp, S.I. *Science* **2001**, *294*, 1684–1688.
(7) Capito, R.M.; Azevedo, H.S.; Velichko, Y.S.; Mata, A.; Stupp, S.I. *Science* **2008**, *319*, 812–816.
(8) (a) Ulijn, R.V.; Smith, A.M. *Chem. Soc. Rev.* **2008**, *37*, 664–675. (b) Smith, A.M.; Williams, R.J.; Tang, C.; Coppo, P.; Collins, R.F.; Turner, M.L.; Saiani, A.; Ulijn, R.V.

Adv. Mater. **2008**, *20*, 37–41. (c) Williams, R.J.; Smith, A.M.; Collins, R.; Hodson, N.; Das, A.K.; Ulijn, R.V. *Nat. Nanotech.* **2009**, *4*, 19–24. (d) Xu, H.; Das, A.K.; Horie, M.; Shaik, M.S.; Smith, A.M.; Luo, Y.; Lu, X.; Collins, R.; Liem, S.Y.; Song, S.; Popelier, P.L.A.; Turner, M.L.; Xiao, P.; Kinloch, I.A.; Ulijn, R.V. *Nanoscale* **2010**, *2*, 960–966. (e) Sadownik, J.W.; Ulijn, R.V. *Chem. Commun*. **2010**, *46*, 3481–3483. (f) Tang, C.; Smith, A.M.; Collins, R.F.; Ulijn, R.V.; Saiani, A. *Langmuir* **2009**, *25*, 9447–9453. (g) Saiani, A.; Mohammed, A.; Frielinghaus, H.; Collins, R.; Hodson, N.; Kielty, C.M.; Sherratt, M.J.; Miller, A.F. *Soft Matter.* **2009**, *5*, 193–202. (h) Guilbaud, J.-B.; Vey, E.; Boothroyd, S.; Smith, A.M.; Ulijn, R.V.; Saiani, A.; Miller, A.F. *Langmuir* **2010**, *26*, 11297–11303.

(9) (a) Rehm, T.H.; Schmuck, C. *Chem. Soc. Rev.* **2010**, *39*, 3597–3611. (b) Woolfson, D.N.; Ryadnov, M.G. *Curr. Opin. Chem. Biol*. **2006**, *10*, 559–567. (c) Gribbon, C.; Channon, K.J.; Zhang, W.; Banwell, E.F.; Bromley, E.H.C.; Chaudhuri, J.B.; Oreffo, R.O.C.; Woolfson, D.N. *Biochemistry* **2008**, *47*, 10365–10371. (d) Holmstr, S.C.; King, P.J.S.; Ryadnov, M.G.; Butler, M.F.; Mann, S.; Woolfson, D.N. *Langmuir* **2008**, *24*, 11778–11783. (e) Papapostolou, D.; Bromley, E.H.C.; Bano, C.; Woolfson, D.N. *J. Am. Chem. Soc*. **2008**, *130*, 5124–5130. (f) Banwell, E.F.; Abelardo, E.S.; Adams, D.J.; Birchall, M.A.; Corrigan, A.; Donald, A.M.; Kirkland, M.; Serpell, L.C.; Butler, M.F.; Woolfson, D.N. *Nat. Mater.* **2009**, *8*, 596–600. (g) Ryadnov, M.G.; Bella, A.; Timson, S.; Woolfson, D.N. *J. Am. Chem. Soc*. **2009**, *131*, 13240–13241. (h) Channon, K.J.; Devlin, G.L.; MacPhee, C.E. *J. Am. Chem. Soc.* **2009**, *131*, 12520–12522. (h) Woolfson, D.N. *Biopolymers* (*Pept. Sci.*) **2010**, *94*, 118–127.

(10) (a) Yan, X.; Zhua, P.; Li, J. *Chem. Soc. Rev.* **2010**, *39*, 1877–1890. (b) Zhu, P.; Yan, X.; Su, Y.; Yang, Y.; Li, J. *Chem. Eur. J.* **2010**, *16*, 3176–3183. (c) Yan, X.; He, Q.; Wang, K.; Duan, L.; Cui, Y.; Li, J. *Angew. Chem. Int. Ed*. **2007**, *46*, 2431–2434. (d) Yan, X.; Cui, Y.; He, Q.; Wang, K.; Li, J. *Chem. Mater.* **2008**, *20*, 1522–1526.

(11) (a) Zhao, X.; Zhang, S. *Chem. Soc. Rev.* **2006**, 35, 1105–1110. (b) Gelain, F.; Horii, A.; Zhang, S. *Macromol. Biosci*. **2007**, *7*, 544–551. (c) Gelain, F.; Lomander, A.; Vescovi, A.L.; Zhang, S.J. *Nanosci. Nanotechnol*. **2007**, *7*, 424–434.

(12) Reches, M.; Gazit, E. *Science* **2003**, *300*, 625–627.

(13) (a) Görbitz, C.H. *Chem. Commun*. **2006**, 2332–2334. (b) Görbitz, C.H.; Nilsen, M.; Szeto, K.; Tangen, L.W. *Chem. Commun*. **2005**, 4288–4290. (c) Görbitz, C.H. *Chem. Eur. J*. **2007**, *13*, 1022–1031. (d) Görbitz, C.H. *Chem. Eur. J*. **2001**, *7*, 5153–5159.

(14) Gazit, E. *Chem. Soc. Rev.* **2007**, *36*, 1263–1269.

(15) (a) Bowerman, C.J.; Ryan, D.M.; Nissan, D.A.; Nilsson, B.L. *Mol. BioSyst*. **2009**, *5*, 1058–1069. (b) Bowerman, C.J.; Nilsson, B.L. *J. Am. Chem. Soc*. **2010**, *132*, 9526–9527.

(16) Keten, S.; Xu, Z.; Ihle, B.; Buehler, M.J. *Nat. Mater.* **2010**, *9*, 359–367.

(17) Shoulders, M.D.; Raines, R.T. *Annu. Rev. Biochem.* **2009**, *78*, 929–958.

(18) Doherty, G.J.; McMahon, H.T. *Annu. Rev. Biophys.* **2008**, *37*, 65–95.

(19) Kreplak, L.; Doucet, J.; Dumas, P.; Briki, F. *Biophys. J.* **2004**, *87*, 640–647.

(20) Dobson, C.M. *Nature* **2003**, *426*, 884–890.

(21) (a) Whitesides, G.M.; Grzybowski, B. *Science* **2002**, *295*, 2418–2421. (b) Dankers, P.Y.W.; Meijer, E.W. *Bull. Chem. Soc. Jpn* **2007**, *80*, 2047–2073. (c) Palmer, L.C.; Newcomb, C.J.; Kaltz, S.R.; Spoerke, E.D.; Stupp, S.I. *Chem. Rev.* **2008**, *108*, 4754–4783.

(22) Avinash, M.B.; Govindaraju, T. *Nanoscale* **2011**, *3*, 2536–2543.

(23) (a) Kim, D.-H.; Viventi, J.; Amsden, J.J.; Xiao, J.; Vigeland, L.; Kim, Y.-S.; Blanco, J.A.; Panilaitis, B.; Frechette, E.S.; Contreras, D.; Kaplan, D.L.; Omenetto, F.G.; Huang, Y.; Hwang, K.-C.; Zakin, M.R.; Litt, B.; Rogers, J.A. *Nat. Mater.* **2010**, *9*, 511–517. (b) Sahni, V.; Blackledge, T.A.; Dhinojwala, A. *Nat. Commun*. **2010**, *1*, 1–4. (c) Lv, S.; Dudek, D.M.; Cao, Y.; Balamurali, M.M.; Gosline, J.; Li, H. *Nature* **2010**, *465*, 69–73. (d) Knowles, T.T.P.J.; Oppenheim, W.; Buell, A.K.; Chirgadze, D.Y.; Welland, M.E. *Nat. Nanotech*. **2010**, *5*, 204–207.

(24) Tracz, S.M.; Abedini, A.; Driscoll, M.; Raleigh, D.P. *Biochemistry* **2004**, *43*, 15901–15908.

(25) (a) Corey, R.B. *J. Am. Chem. Soc*. **1938**, *60*, 1598–1604. (b) MacDonald, J.C.; Whitesides, G.M. *Chem. Rev.* **1994**, *94*, 2383–2420.

(26) (a) Palacin, S.; Chin, D.N.; Simanek, E.E.; MacDonald, J.C.; Whitesides, G.M.; McBride, M.T.; Palmore, G.T.R. *J. Am. Chem. Soc*. **1997**, *119*, 11807–11816. (b) Palmore, G.T.T.; McBride, M.T. *Chem. Commun*. **1998**, 145–146. (c) Palmore, G.T.R.; Luo, T.-J.M.; McBride-Wieser, M.T.; Picciotto, E.A.; Reynoso-Paz, C.M. *Chem. Mater.* **1999**, *11*, 3315–3328. (d) Chin, N.; Palmore, G.T.R.; Whitesides, G.M. *J. Am. Chem. Soc*. **1999**, *121*, 2115–2122. (e) Luo, T.-J.M.; Palmore, G.T.R. *J. Phys. Org. Chem*. **2000**, *13*, 870–879. (f) Du, Y.; Creighton, C.J.; Tounge, B.A.; Reitz, A.B. *Org. Lett*. **2004**, *6*, 309–312.

(27) (a) Mendham, A.P.; Palmer, R.A.; Potter, B.S.; Dines, T.J.; Snowden, M.J.; Withnalld, R.; Chowdhry, B.Z. *J. Raman Spectrosc*. **2010**, *41*, 288–302. (b) Benedetti, E.; Corradini, P.; Pedone, C. *J. Phys. Chem*. **1969**, *73*, 2891–2895. (c) Sletten, E. *J. Am. Chem. Soc*. **1970**, *92*, 172–177. (d) Sletten, J. *Acta Chem. Scand. A* **1980**, *34*, 593–595. (e) Cheam, T.C.; Krimm, S. *Spectrochim. Acta* **1988**, *44A*, 185–208.

(28) Bergeron, R.J.; Phanstiel IV, O.; Yao, G.W.; Milstein, S.; Weimar, W.R. *J. Am. Chem. Soc.* **1994**, *116*, 8479–8484.

(29) Joshi, K.B.; Verma, S. *Tetrahedron Lett.* **2008**, *49*, 4231–4234.

(30) Adler-Abramovich, L.; Aronov, D.; Beker, P.; Yevnin, M.; Stempler, S.; Buzhansky, L.; Rosenman, G.; Gazit, E. *Nat. Nanotech.* **2009**, *4*, 849–854.

(31) Govindaraju, T.; Pandeeswar, M.; Jaipuria, G.; Atreya, H.S. *Supramol. Chem.* **2011**, *23*, 487–492.

(32) (a) Machin, P.J.; Sammes, P.G. *J. Chem. Soc. Perkin Trans.* **1976**, *1*, 624–627. (b) Schkeryantz, J.M.; Woo, J.C.G.; Siliphaivanh, P.; Depew, K.M.; Danishefsky, S.J. *J. Am. Chem. Soc*. **1999**, *121*, 11964–11975.

(33) Martins, M.B.; Carvalho, I. *Tetrahedron* **2007**, *63*, 9923–9932.

(34) Ivanova, B.B. *Spectrochim. Acta A* **2006**, *64*, 931–938.

(35) Silvester, M.F.; Yannas, I.V.; Forbes, M.J. *Tromb. Res.* **1989**, *55*, 135–148.

(36) Yannas, I.V. Natural Materials. In *Biomaterials Science: An Introduction to Materials in Medicine*; Ratner, B.D., Hoffman, A.S., Schoen, F.J., Lemons, J.E., Eds., 2nd ed.; Chap. 1; Elsevier: San Diego, CA, 2004; pp 127–137.

(37) Piepenbrock, M.-O.M.; Clarke, N.; Steed, J.W. *Soft Matter.* **2010**, *6*, 3541–3547.

(38) Kopple, K.D.; Marr, D.H. *J. Am. Chem. Soc.* **1967**, *89*, 6193–6200.

(39) Gdaniec, M.; Liberek, B. *Acta Cryst.* **1986**, *C42*, 1343–1345.